JOURNAL OF GEOPHYSICAL RESEARCH, VOL. 103, NO. C6, PAGES 12,709–12,724, JUNE 15, 1998

Greenland Sea Odden sea ice feature: Intra-annual and interannual variability

Robert A. Shuchman,[1] Edward G. Josberger,[2] Catherine A. Russel,[1]
Kenneth W. Fischer,[1] Ola M. Johannessen,[3] Johnny Johannessen,[4] and Per Gloersen[5]

Abstract. The "Odden" is a large sea ice feature that forms in the east Greenland Sea that may protrude eastward to 5°E from the main sea ice pack (at about 8°W) between 73° and 77°N. It generally forms at the beginning of the winter season and can cover 300,000 km^2. Throughout the winter the outer edge of the Odden may advance and retreat by several hundred kilometers on timescales of a few days to weeks. Satellite passive microwave observations from 1978 through 1995 provide a continuous record of the spatial and temporal variations of this extremely dynamic phenomenon. Aircraft synthetic aperture radar, satellite passive microwave, and ship observations in the Odden show that the Odden consists of new ice types, rather than older ice types advected eastward from the main pack. The 17-year record shows both strong interannual and intra-annual variations in Odden extent and temporal behavior. For example, in 1983 the Odden was weak, in 1984 the Odden did not occur, and in 1985 the Odden returned late in the season. An analysis of the ice area and extent time series derived from the satellite passive microwave observations along with meteorological data from the International Arctic Buoy Program (IABP) determined the meteorological forcing associated with Odden growth, maintenance, and decay. The key meteorological parameters that are related to the rapid ice formation and decay associated with the Odden are, in order of importance, air temperature, wind speed, and wind direction. Oceanographic parameters must play an important role in controlling Odden formation, but it is not yet possible to quantify this role because of a lack of long-term oceanographic observations.

1. Introduction

For centuries, Scandinavian fishermen and sealers have reported the occurrence of the "Odden," a rapid eastward advance of the sea ice in the East Greenland Sea, as it trapped their vessels. The Odden is a large tongue of sea ice, centered between 73° and 77°N, that curves northeastward into the center of the Greenland Sea. The Odden curves around a body of open water to the north known as the "Nordbukta." Typically, the Odden begins to form early in the winter at around 8°W between 72° and 74°N and can eventually extend northeastward to about 5°E. In addition, the edge of the Odden can rapidly expand and contract by as much as 200 km in periods as short as 4-6 days or may stay in an extended configuration for a month or more. *Bourke et al.* [1992] showed that the Odden is influenced by the Jan Mayen Polar Current, which has surface waters that are cold and fresh and hence more readily subject to freezing. A schematic drawing of the currents surrounding the Odden study area is shown in Figure 1. This study of the Odden ice formation seeks to provide insight into the complex interactions of atmosphere, ice, and ocean in this region of the Greenland Sea that govern the formation and decay of the Odden.

[1]ERIM International Inc., Ann Arbor, Michigan.
[2]Ice and Climate Project, United States Geological Survey, University of Puget Sound, Tacoma, Washington.
[3]Nansen Environmental and Remote Sensing Center, Bergen, Norway.
[4]European Space Research and Technology Centre, European Space Agency, Noordwijk, Netherlands.
[5]NASA Goddard Space Flight Center, Greenbelt, Maryland.

Paper number 98JC00375.
0148-0227/98/98JC-00375$09.00

The large-scale and rapid variations of the Odden indicate that it plays an important role in the dynamics and the heat and salt budgets of the Greenland Sea. *Aagaard and Carmack* [1989] describe the complex interactions of the polar and Atlantic water masses that interact with each other and the large-scale circulation in the Greenland Sea. These interactions determine the deep ocean ventilation and subsequent distribution of the new water masses. During the winter, the eastward extent of the ice edge (and the Odden) is limited by the location of the Polar Front. This front separates polar water (T<0°C and S<34.5 practical salinity units (psu)) from Atlantic water types (T>2°C, S>34.9 psu) and generally trends north-south. *Hopkins* [1988] describes 35 water types in this area that result from the various mixing processes that occur, including the irreversible changes that result from ice formation and melting, and he also gives a comprehensive review of the circulation in the Greenland-Iceland-Norwegian (GIN) Sea. *Van Aken et al.* [1991] give a detailed description of the complex frontal systems found along a section line at 74°45' N, from 10°W to 17°E during February of 1989. The complexity probably results from the advance and retreat of the Odden through this area, although the two features are interdependent and the causality of the relationship is uncertain.

The Odden ice is also believed to play a key role in controlling deep water formation in the Greenland Sea through the process of deep water convection [*Killworth*, 1979; *Schott et al.*, 1993; *Paluszkiewicz et al.*, 1994]. More than 85% of the deep water formed in the oceans occurs in < 5% of its surface area. This small area is located predominantly in high-latitude areas including the Labrador, Greenland, and Mediterranean Seas in the northern hemisphere and the Ross and Weddell Seas in the southern hemisphere. There is a possibility that occurrences of deep convection oscillate between the Labrador and Greenland

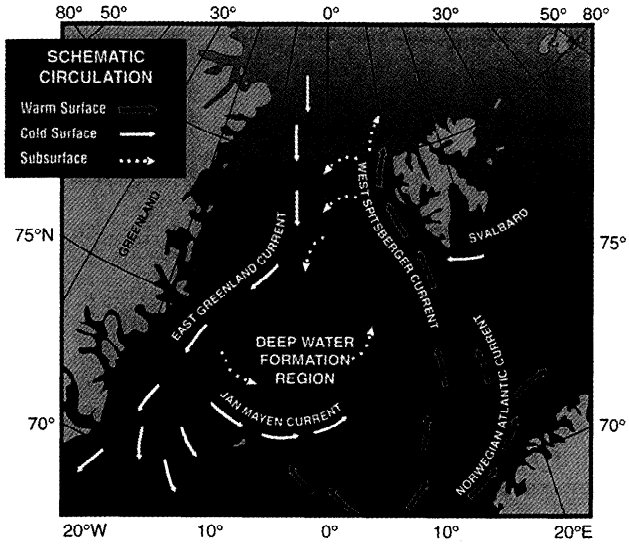

Figure 1. Ocean circulation patterns in the Greenland Sea influencing Odden formation.

Seas in response to shifting atmospheric conditions. In particular, *Visbeck et al.* [1995] suggest that the primary Greenland Sea deep water (GSDW) formation site is located in the Nordbukta open water region. The Odden ice cover in the Greenland Sea strongly regulates deep water convection by limiting the strong surface cooling needed for convection, and conversely, by increasing upper layer salinity through injection of brine into the surface mixed layer during the ice formation process. *Schlosser et al.* [1991] related changes of concentrations of chlorofluorocarbons and tritium in GSDW to deep water formation from 1972 to 1989. A box model showed that bottom water formation decreased by 80% some time in the period between 1978 and 1982 and has persisted to 1989. The reduction could be the result of a salinity anomaly in the GIN Sea reaching the Fram Strait area in ~1980 [*Dickson et al.*, 1988]. This time period also corresponds to a minimum in potential temperature found by *Alekseev et al.* [1994].

Despite its great extent and high variability, the relation of the Odden to processes that occur in the GIN Sea is poorly understood. This study uses synthetic aperture radar (SAR) to provide high resolution "truth" to validate the coarser sea ice classification derived from the satellite passive microwave observations. Time series of Odden ice area and extent, developed from the scanning multichannel microwave radiometer (SMMR) and the special sensor microwave imager (SSM/I) passive microwave data sets, are combined with meteorological data from the University of Washington Polar Science Center International Arctic Buoy Program (IABP) to address the issue of meteorological forcing of Odden ice formation. The Odden and its rapid variations were first observed by satellite passive microwave during the period 1973-76 using the electrically scanning microwave radiometer (ESMR) on board Nimbus 5 [*Parkinson et al.*, 1987]. Odden ice area and extent from the period 1978-1987 have been described in earlier publications [*Gloersen et al.*, 1992]. *Wadhams et al.* [1996] give a detailed study of the 1993 Odden. This paper extends the period of observation to 1995 and performs a statistical analysis of Odden growth, decay, or stagnation and of temperature, wind speed and direction, and pressure forcing. Finally, longer-term cycles and trends in the Odden ice area are discussed in terms of interannual variability. The lack of repetitive, synoptic, oceanographic data from the Greenland Sea prevents a similar detailed analysis of the atmosphere-ice-ocean interactions.

2. Data Sets and Odden Observations

This study used aircraft synthetic aperture radar (SAR) observations of the Odden to verify the satellite passive microwave observations of Odden conditions. This verification was necessary because the ice in the Odden consists of large amounts of new ice types, whose passive microwave signatures are not completely understood [*Shuchman and Onstott*, 1990; *Eppler et al.*, 1992; *Grenfell et al.*, 1992; *Campbell et al.*, 1994; *Toudal*, 1994]. In situ ship and scatterometer observations provide the basis for interpreting the SAR observations, especially of new ice types, and for extending the interpretation to the passive microwave observations. Coincident meteorological data for this study were provided through the use of drifting buoys deployed in the Arctic. Each of these data sets will be described below.

2.1. Satellite Passive Microwave Observations

Plate 1 shows an example of the structure and location of the Odden event as derived from satellite passive microwave observations. The highlighted area from 70° to 79°N and 20°W to 6°E encompasses the Odden and was the area used for the microwave analysis. The Odden is easily distinguished from the rest of the ice pack in part because of its location and shape and also, in sequential images, because of its rapid formation and dissipation. The Odden appears as the large ice protrusion off the main ice pack on the east coast of Greenland and extends northeastward toward Svalbard. The ice concentration estimates show the Odden as a thumb-like feature with the highest ice concentrations at the center of the feature and lower concentrations at the edges.

2.1.1. SMMR and SSM/I data sets. The SMMR and SSM/I satellite passive microwave sensors have provided all-weather, all-season imagery of global sea ice from 1978 to the present. While both of these sensors provide low-resolution imagery (50 km), the Odden event can clearly be seen in the imagery because of its large size (up to 300,000 km^2 in area). Plate 2 shows an example of eight ice concentration maps derived from the Nimbus 7 SMMR observations of the Greenland Sea for a 1-month period between March 21 and April 18, 1987, and shows a sudden retreat followed by an advance of the ice edge and then another retreat. Because of the ability to clearly identify the Odden without interference of cloud cover or darkness and because the data are available on a near daily basis since 1978, the SMMR and SSM/I provide a unique 17-year-long continuous record of Odden conditions in the Greenland Sea. *Cavalieri et al.* [1984] give a complete description of the SMMR instrument, and a similar description of SSM/I can be found in work by *Hollinger* [1989] and in *the National Snow and Ice Data Center (NSIDC)* [1992] user's guide.

The SMMR instrument, carried on board the Nimbus 7 satellite, collected data on a daily basis from October 1978 to November 1978, and on a alternate-day basis from November 1978 to August 1987 because of spacecraft power limitations [*Gloersen and Barath*, 1977; *Gloersen et al.*, 1992]. The orbital inclination and swath width of the SMMR sensor did not allow for mapping of areas poleward of 84°N, and hence there is a data hole around both poles. This data gap, however, is well north of

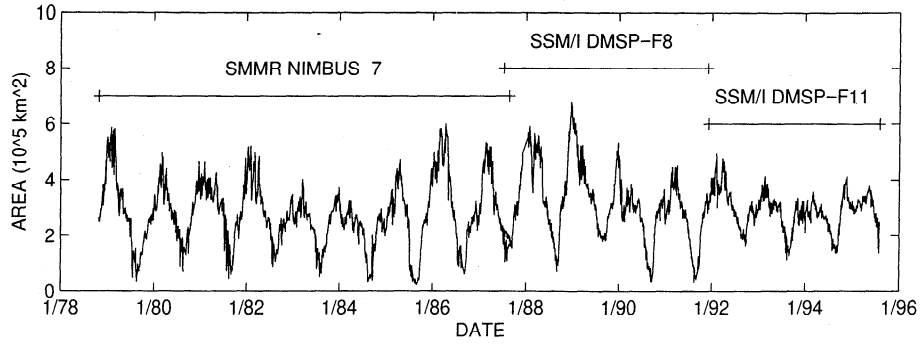

Figure 2. Total sea ice area in the Greenland Sea as a function of year for the SMMR and SSM/I 17-year history.

the area considered in this analysis. The SSM/I sensor, which is operated on board a series of Defense Meteorological Satellite Program (DMSP) spacecraft, has provided complete daily coverage of the polar region (with a similar data gap poleward of 87°N) since July 1987 and continues to collect data.

The SMMR and SSM/I brightness temperatures used to calculate total ice concentrations were taken from CD-ROMs distributed by NSIDC, in Boulder, Colorado. Potentially higher quality reanalyzed versions of the same data sets are also available from the European Centre for Medium-Range Weather Forecasts (ECMWF) and from the National Center for Environmental Prediction (NCEP), although it is not believed that the minor differences in these data sets would substantially alter the results of this study. Both sets of CD-ROMs contain daily (SSM/I) and bidaily (SMMR) gridded brightness temperature (T_b) values for all channels that the sensors operate. The T_b values used in deriving total ice concentration (18-GHz horizontal-polarization (H), 18-GHz vertical-polarization (V), and 37-GHz V for the SMMR and 19-GHz H, 19-GHz V, and 36-GHz V for the SSM/I) were binned into a polar stereographic projection with a fixed grid cell size of 25 by 25 km. For a complete description of the processing steps taken to produce the gridded brightness temperature data sets, see works by NSIDC [1992, 1994]. Although *Wadhams et al.* [1996] showed that there was good agreement between the derived ice edge using ERS-1 and from the 85-GHz channel from the SSM/I, this channel was not used in this analysis because it was not carried by the SMMR and is strongly affected by cyclonic activity.

It should be noted that the NSIDC products are based on averages over 24 hours, a period of sufficient duration that the Odden may vary significantly in extent between samples. In the case where the SMMR data were only available every other day, there is up to 48 hours between images. Ideally for this analysis, the sampling should be more frequent, perhaps every 12 hours, to correspond with the meteorological data described in section 2.3. Nonetheless, for the timescales of the analysis performed here, the data have proven to be adequate.

The algorithm for calculating the sea ice concentrations, such as those shown in Plates 1 and 2 uses multispectral radiances obtained from SMMR and SSM/I. This study used the algorithm developed by the NASA Sea Ice Algorithm Working Team [*Gloersen et al.*, 1984; *Cavalieri et al.*, 1984; *Gloersen and Cavalieri*, 1986] to calculate total ice concentration and multiyear ice fraction from both sensors. The NASA Team algorithm was selected because it has been sufficiently validated in numerous studies using both in situ data measurements, and other remotely sensed data such as SAR and Landsat (see also section 2.2). For reference, the tie points used in deriving sea ice concentration for this analysis can be found in the NSIDC user's guides for the SMMR and SSM/I brightness temperature and sea ice concentration grids [*NSIDC*, 1992, 1994]. For this analysis, the total ice concentration values, as derived from the SMMR and SSM/I using the NASA Team algorithm, provided the estimates of ice coverage in the Odden event.

Cavalieri et al. [1984] estimate that the sea ice concentration calculations have an accuracy of about 5% in the central pack and about 9% in the marginal ice zone, where as much as 30% of the ice may be thin or new and without snow cover (two ice types not taken explicitly into account by the algorithm). In the case of the Odden ice which has been shown to contain mostly new ice types [*Wadhams et al.*, 1996], the accuracy may be substantially poorer than 9%. The error in ice area determination could be larger yet if the ice is pancake ice, which can be partially flooded and would appear as open water. Since the brightness temperatures are sensitive to ice type and flooding/draining that can vary rapidly with time, this may also affect the repeatability of the algorithm results. Measurement accuracies can also be affected by wind-induced ocean surface roughness, atmospheric water vapor, and cloud liquid water. The results presented later in this paper are based primarily on changes in ice area and hence are only weakly dependent on absolute accuracies of the ice area estimation. The precision or repeatability of the ice coverage calculations is probably better than the accuracy, i.e., closer to the value expected on the basis of instrument noise and drift, (1-2% for a single footprint).

2.1.2. SMMR and SSM/I Odden observations. The 17-year SMMR and SSM/I record provides a continuous time series of the total sea ice area in the Greenland Sea as shown in Figure 2; large seasonal and annual variations are very pronounced. The higher-frequency fluctuations in the winter months (i.e., on a weekly and monthly scale) represent sea ice area changes of up to 300,000 km^2 that are Odden events. Figures 3a and 3b show the yearly time series of the Odden ice area as derived from the SMMR and SSM/I. The winter of 1994-1995 was not shown because all values of Odden ice area were zero. This time series will be discussed in more detail in section 4.

To calculate the amount of Odden ice using the SMMR and SSM/I passive microwave data sets, the initial ice-covered area in the Greenland Sea study area for each year was established and then subtracted from the daily ice concentration maps. The initial state for each year was determined by averaging all of the total ice concentration estimates for the month of October for each year to produce an average "pre-Odden" ice concentration map for that year. October was chosen for calculating the initial

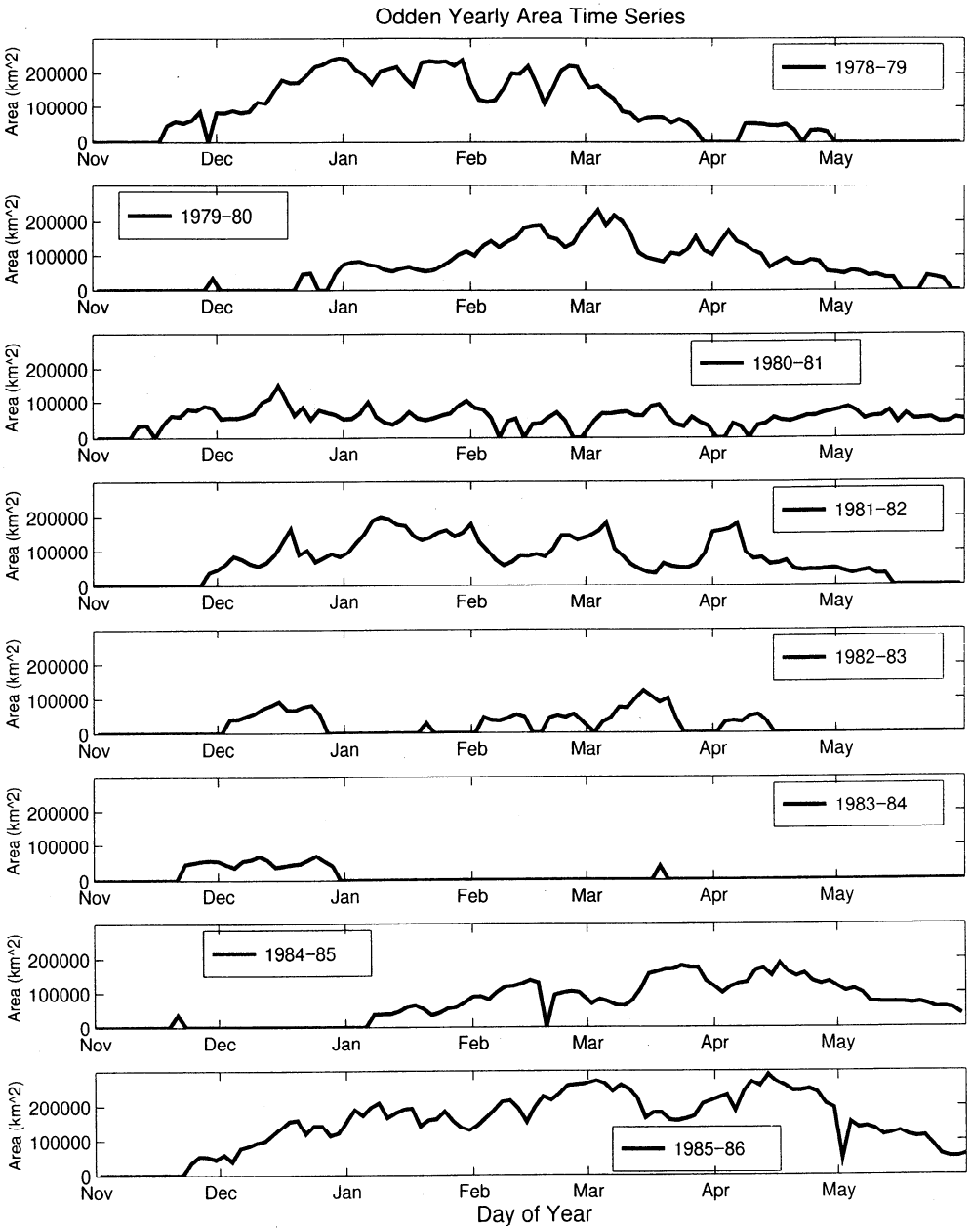

Figure 3a. Yearly time series of Odden area derived from SMMR data covering winters 1978-1979 through 1985-1986.

winter ice edge because this is approximately the time of minimum ice extent, and the Odden generally does not begin to form until November or later.

Annual time series of sea ice extent and total ice-covered area for the Odden region (70°-79°N and 20°W-6°E) were calculated from the daily maps and the October average conditions. The Odden ice extent was derived by summing the areas of the pixels with at least 30% ice concentration [*Wackerman et al.*, 1988] beyond the derived winter ice edge in the defined Odden region. The Odden ice area was derived by summing the total ice concentration for a pixel times the pixel area.

2.2. Aircraft SAR and In Situ Observations

The second set of data used for this study was the airborne synthetic aperture radar (SAR) imaged, ship-based meteorological measurements and ice data collected during the 1987 Marginal Ice Zone Experiment (MIZEX '87). Two research vessels operated during MIZEX '87: the ice-strengthened R/V *Polar Circle* and the open water *Håkon Mosby*. Both ships made meteorological measurements and conductivity-temperature-depth (CTD) sections in the area of the Odden. Ice samples of the Odden were obtained by R/V *Polar Circle*. A complete description of the in situ MIZEX '87 measurements is discussed in the report by the MIZEX '87 Group [1989]. The Fram Strait operating area for MIZEX '87 extended along the ice edge from about 75° to 79°N and 5°W to 5°E. Although the majority of the MIZEX '87 study area was north of the typically assumed Odden area, the southern portion of the MIZEX study region covers the northern portion of the Odden, and the data collected during MIZEX provide important in situ and high-resolution remotely sensed information on the new ice types found in the Odden. The ice types contained in the northern

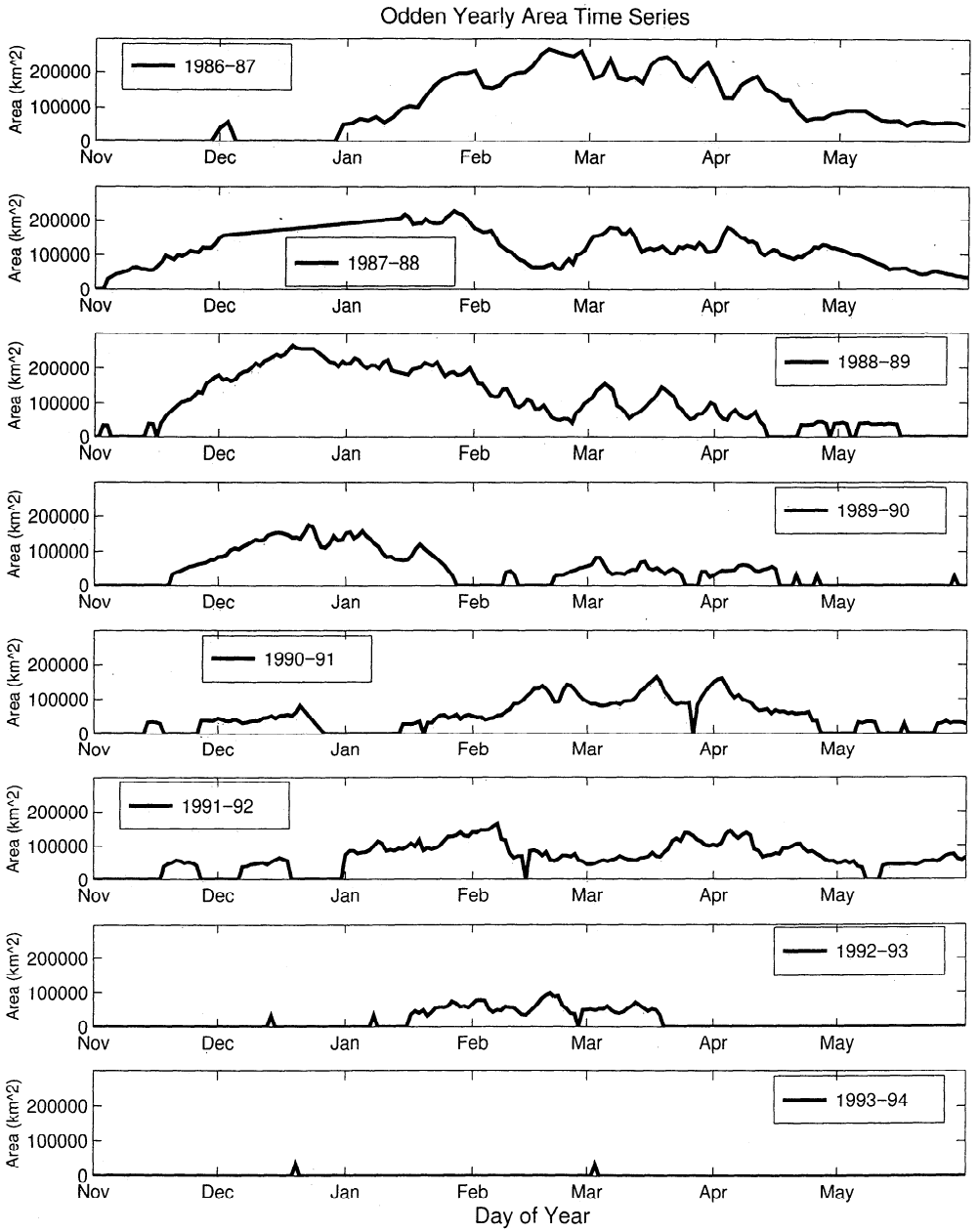

Figure 3b. Yearly time series of Odden area derived from SMMR and SSM/I data covering winters 1986-1987 through 1993-1994. Note that 1994-1995 was not shown since all values were zero.

extent of the Odden along with their radiometric properties were determined by scientists on board the *Polar Circle* and *Håkon Mosby*. The northernmost portion of the Odden advances and retreats was imaged by an airborne X-band SAR.

The aircraft SAR provided detailed ice imagery in the area bounded by 75° to 80°N and 10°W to 10°E, and *Shuchman et al.* [1988] describe this system. The SAR data were digitally processed on board the aircraft and transmitted to shipboard scientists directing the experiment. Mosaics of the SAR data were then generated and manually/digitally interpreted with respect to ice type, concentration, and floe size distribution [*Shuchman et al.*, 1989]. A complete description of the SAR analysis is given by *Campbell et al.* [1987]. The accuracies of the SAR interpretations are ~5% with respect to concentration and floe size distributions.

The SMMR observations of the area between 70° and 84°N during the period of March 15 through April 15, 1987, corresponding to the time the SAR and *Polar Circle* were deployed in the Odden area, showed that a major Odden event took place. Plate 2 shows eight SMMR ice concentration maps that show a sudden retreat of the ice edge followed by an advance and another retreat between March 21 and April 18, 1987. During the first 4 days of April the Odden decreased significantly in area and then grew to a maximum on April 10 and once again decreased in size. During the period March 29 through April 10, six aircraft SAR images of ice conditions in the northern portion of the Odden were obtained on even Julian days corresponding to SMMR observations [*O.M. Johannessen et al.*, 1994]. The SAR data showed that the SMMR-derived ice concentration and extent values based on the NASA Team algorithm were accurate when

the 30% SMMR-derived ice concentration line was used to represent the ice edge. Specifically, the SMMR and SAR ice edges agree to within 25 km of each other, well within the 50-km resolution of the 19-GHz channels of the SMMR sensor. Also, the 90% SMMR concentration lines are consistent with the SAR-reported 95% line, and the 50-70% SMMR values correspond well to the SAR estimates of 50-60%.

Ship observations of the ice in the northern portion of the Odden area showed that the sea ice consisted of 100% granular pancake floes 20-30 cm thick, with a bulk salinity of ~10.5 psu and a density of 0.92 Mg m^{-3}. *Tucker et al.* [1991] describe a suite of active and passive microwave measurements of this pancake ice that were made on March 29 at 78°50' N and 1°40' E. The passive measurements obtained at 7, 11, 18, 21, and 37 GHz at an incidence angle of 40° showed good separation between the brightness temperatures from the Odden ice and the surrounding open water.

On April 4, 1987, in situ observations of the Odden ice were also made from the *Polar Circle*. On this day in the approximate area of 76°30' N and 2°W (the northern portion of the Odden) the ice consisted of 100% granular nilas, 3 cm thick with bulk salinity of ~15.3 psu and a density of 0.92 Mg m^{-3}. For reference, the SMMR-derived ice concentration at this location and time was 20-30%.

In analyzing the northern part of the Odden between March 29 and April 2, using SMMR-derived ice concentrations, the ice edge decayed by ~200 km (see Plate 2). This was followed by a rapid 100-130-km advance of ice in the 2-day period between April 4 and April 6. If only wind drift was responsible for the ice edge advance, then the eastward ice drift would be of the order of 50-75 cm s^{-1}, which is unusually high. To attain these high drift rates, a free ice drift model requires wind speeds of between 25 and 37 m s^{-1}. The local wind conditions during the event reveal that the maximum wind speed was 15 m s^{-1}, and blowing off the ice from a northwesterly direction. Thus the only explanation is the rapid ice formation off the main ice edge. This is supported by the SAR and ship observations. Oceanographic and meteorological observations, combined with the preponderance of new ice types within the Odden, suggest that the Odden is the result of ice formation rather than ice advection out from the main pack along the Greenland coast.

2.3. Meteorological Data Sets

While the SMMR and SSM/I data sets provided long-term estimates of the Odden occurrence and its areal coverage, drifting buoys deployed in the Arctic provided the necessary coincident meteorological data for this analysis. The International Arctic Buoy Program (IABP) currently maintains a network of drifting buoys. Processed data sets from the University of Washington Polar Science Center provide atmospheric pressure and air temperature estimates at the sea ice surface [*Colony and Rigor*, 1995]. The buoy data spanned the time frame from January 1979 through April 1994 (sampled twice daily with temperature data unavailable from January 1991 through April 1993). This data set provided coincident data for the SMMR-and SSM/I-derived ice concentrations. The buoys were deployed on ice floes, and buoy data were transmitted to Service Argos where the data were decoded and processed.

In addition to the data from buoys, IABP combines a variety of data sources to provide accurate meteorologic fields. These sources include surface temperature and pressure values from surface observation stations surrounding the Arctic basin, including Jan Mayen (71°N, 8°W), and for areas north of 70°N but far from any buoys (modeled pressure fields from NCEP). This fusion of buoy, surface station, and modeled data gives an accurate estimate of surface temperature and pressure at a given location for the 16-year record. The gridded data sets of the temperature and pressure were derived with a fixed latitude/longitude sampling north of 70°N with a sample spacing of 2° in latitude and 10° in longitude. Estimates of the temperature and pressure in the general location of the Odden were derived by averaging all grid points in the grid from 71° to 77°N and 15°W to 5°E, six data points in all. Geostrophic wind speed and direction were calculated from the buoy data by calculating the pressure gradient from the gridded pressure data fields. Estimates of the geostrophic wind speed and direction were derived by averaging the six data points contained in the Odden area.

The IABP data suffer from limitations in the sample spacing due to the small number of buoys in the Arctic at any one time, and the paucity of surface observation stations at these high latitudes. Although the year-round ice advection through the Fram Strait often brings buoys into the Odden area, much of the information on meteorological conditions comes from interpolating data from the surface observation stations around the area (Svalbard, Greenland east coast, Jan Mayen, Iceland, and Norway). Hence the IABP data resolve only the relatively large-scale atmospheric circulation. The Odden area is known for small mesoscale activity such as polar lows, which cannot be resolved in the data. These smaller features will likely have significant impacts on short-term ice variability, but the analysis done for this study considers only relatively large ice growth events over 4 days or more which can average over the mesoscale circulations.

Despite the limitations to the quality and resolution of these data, it is the most complete meteorological data set available for this remote region over the 17-year study period. Concerning the air temperature data, in particular, the temperature near the ice boundary is estimated from a combination of onshore temperature and buoy observations. The temperature estimates onshore are hundreds of kilometers away, which can be a source of error in the derivation of offshore air temperature. Also, the buoy temperature data are based on a temperature inside the buoy housing, which may be covered with snow and hence be more representative of snow temperature rather than surface air temperature. For the remainder of the paper, however, these values will be referred to as the surface air temperature. No attempt has been made to further assess the quality of the meteorological data as it is beyond the scope of this study, but it is clear that any conclusions drawn must bear these limitations in mind.

3. Intra-annual Odden Variability

Many questions have been raised regarding the occurrence of the Odden, such as, why does it occur at certain times but not others, and during some years but not others? To address these questions, an analysis was performed using both the remotely sensed ice cover data and the interpolated in situ buoy meteorological data to determine the atmospheric conditions which are associated with the Odden formation, decay, stagnation, or absence. The methodology first identified specific formation and decay events in the time series of ice area coverage, and then compared these events with the meteorology time series to determine which meteorological variables most strongly influence the Odden formation and what, if any,

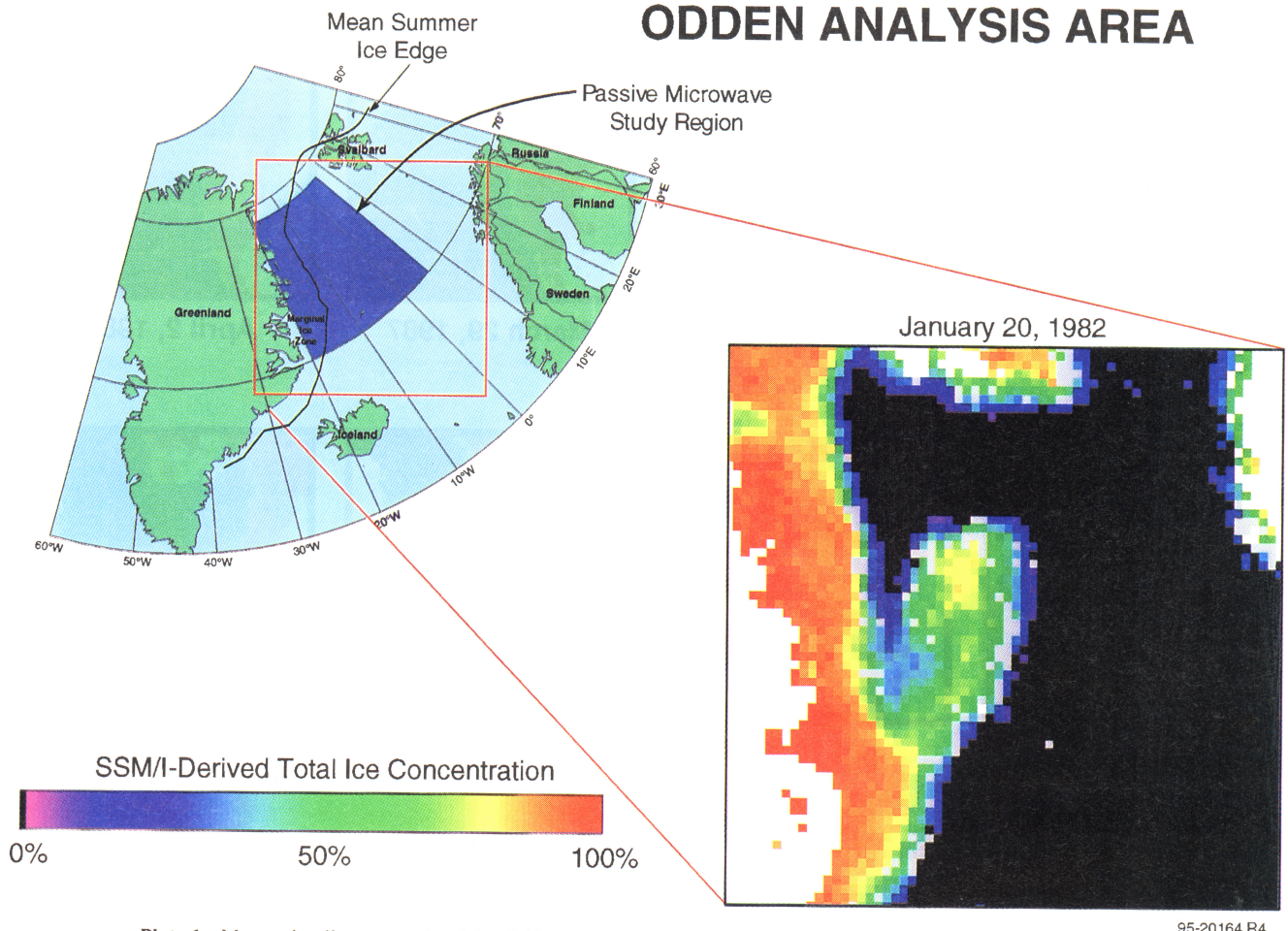

Plate 1. Map and pullout example of the Odden event. The pullout is an SSM/I-derived ice concentration map clearly showing an Odden occurrence off the east coast of Greenland.

thresholds could be identified for triggering an Odden event. The analysis was later broadened to include conditions under which the Odden ice pack maintained itself above certain minimum area levels and when no Odden occurred at all. Once ice formation or decay rate criteria for these periods were selected, specific occurrences of formation, decay, stagnant Odden, and stagnant no-Odden were identified. Statistics on the meteorological conditions during each of these types of occurrences were then compiled to determine which meteorological conditions are most closely associated with Odden formation, maintenance, and decay.

3.1. Identification of Odden Formation and Decay Events

The analysis of intra-annual Odden variability began with the identification of specific periods in the overall SMMR and SSM/I data record, which could be classified as significant growth, significant decay, maintenance of Odden ice pack above a specific area threshold, and no-Odden occurrence. These periods were initially selected visually by inspecting the Odden area and extent times series covering 17 winter seasons derived from SMMR and SSM/I sea ice coverage maps as described in section 2.1. Once these periods had been initially identified, quantitative criteria were established to insure consistent interpretation of the data.

The criteria selected included both a growth or decay rate threshold, and a minimum time period over which the growth or decay rate applied. The growth/decay rates were calculated using the difference between the current and previous data points in the ice area time series. For the case of significant Odden ice growth events, the criterion was a growth rate of >16,000 km^2 d^{-1} over a period of 4 days. On the basis of this criterion, 16 significant growth events covering 66 days were identified. For the case of significant Odden ice decay events, the criterion was a decay rate of > 18,000 km^2 d^{-1} over a period of 4 days. The slightly different threshold for growth and decay events was selected so that approximately the same number of events and days would be used in determining statistics for both cases. On the basis of this criterion, 17 significant decay events covering 64 days were identified.

The criterion used to select periods of nearly steady state Odden conditions, growth, or decay rates averaged over 3 days, was a change of < 3000 km^2 d^{-1} and total ice area exceeding 100,000 km^2 maintained over 3 days or more. The averaging was used to remove high-frequency noise in the data which might indicate large point-to-point variability in the data but did not contribute to a large overall trend. On the basis of these criteria, 11 events covering 200 days were identified where the Odden ice pack area was maintained at significant levels with little or no change over a period of several days. Finally, periods where no Odden activity occurred were identified by stretches where the overall Odden ice area remained below 45,000 km^2, which was the threshold used to decide when any Odden was occurring, for a period of 4 or more days. A total of nine events covering 370 days where there was no-Odden were identified, particularly

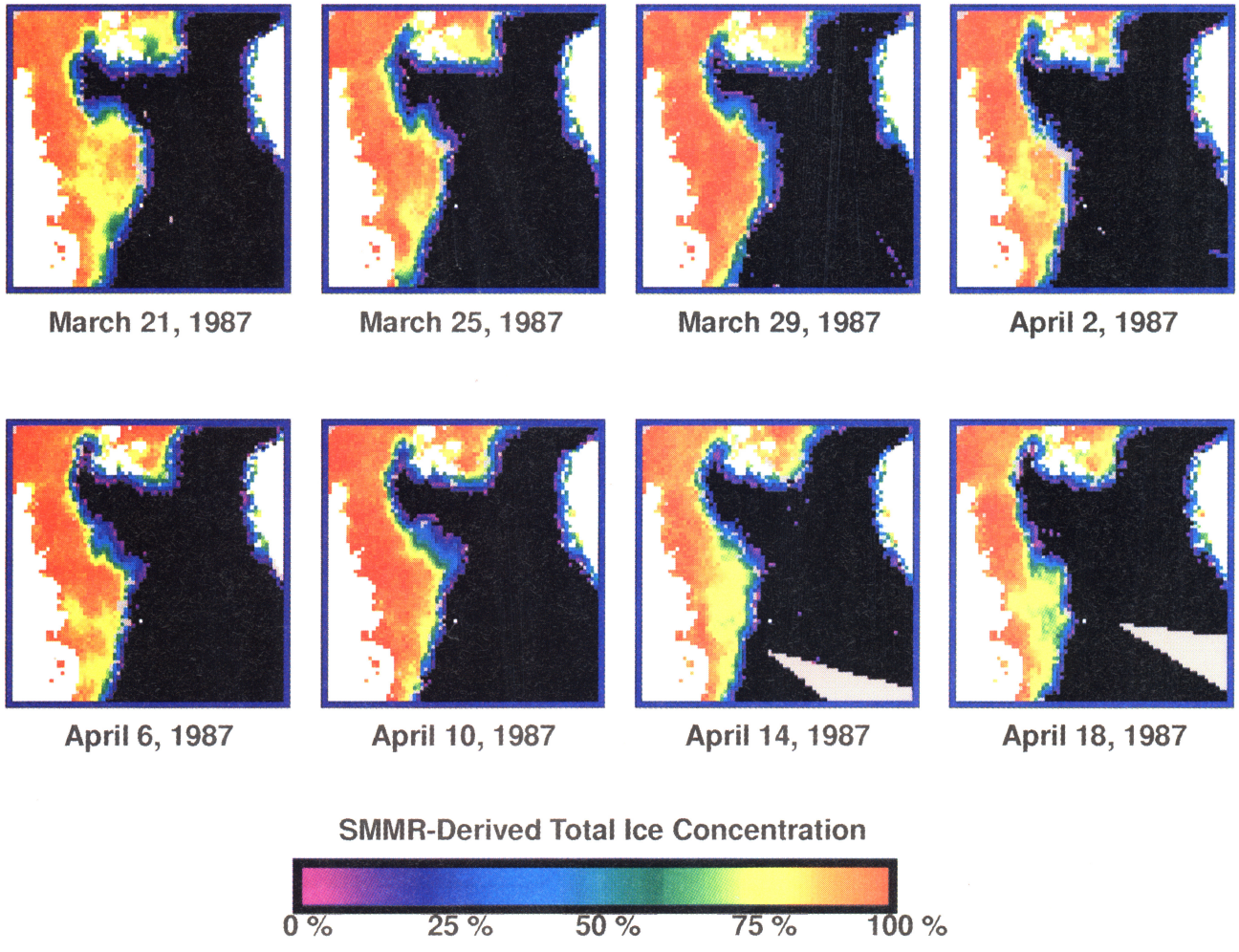

Plate 2. One-month time series from March 21 to April 18, 1987 of ice concentrations derived from the SMMR data collected coincidentally with the MIZEX '87 collection.

during the 1983-1984 and 1993-1994 winter seasons. On the basis of four sets of criteria for Odden ice conditions, approximately one quarter of the data was classified into one of these categories. Once occurrences of these four types of events were identified, the meteorological conditions associated with each type of event were analyzed. To determine the background meteorological climatology on which the Odden occurs, all of the data were averaged together in total and by month.

3.2. Meteorological Conditions Associated With Odden Growth and Decay

As discussed in section 2.3, the meteorological parameters available or derivable from the International Arctic Buoy Program were surface air temperature, surface pressure, and geostrophic wind speed and direction. An analysis was done to determine the meteorological conditions associated with each of the Odden ice cases described in section 3.1. For each case, meteorological data from all of the days fitting the ice criteria were averaged, and standard deviations were calculated. The results of this analysis are summarized in Table 1 and in Figure 4. The parameters are shown ±1 standard deviation in Table 1 to give a sense of the data scatter. Calculation of mean and standard deviation of wind direction presents a unique challenge from a statistical point of view. The method used here for analysis of directional data follows that of *Mardia* [1972], which takes the meridional and zonal components of the wind from a given direction weighted by the frequency of occurrence of that direction.

As can be seen from Table 1, temperature and wind both appear to be related to the Odden ice formation. Atmospheric pressure was not found to be significantly related to any of the ice growth/decay cases and will not be considered here. On the basis of the analysis described below, atmospheric temperature appears to play the most significant role during Odden formation. All of the temperature results make intuitive sense, with the coldest conditions being associated with Odden growth and the warmest being associated with no Odden forming at all. The average temperature required during significant Odden ice

Table 1. Meteorological Conditions

Case/Parameter	Temperature, °C	Wind Speed, m s^{-1}	Wind Direction
Odden growth	-11.7 ± 5.7	7.7 ± 3.9	281.1 ± 51.8
Odden decay	-6.0 ± 4.6	12.4 ± 5.6	3.0 ± 30.5
Stagnant Odden	-9.6 ± 4.8	9.5 ± 5.4	323.0 ± 37.8
Stagnant no-Odden	-2.3 ± 4.8	9.4 ± 5.2	344.5 ± 36.2

Wind direction is in degrees clockwise from north.

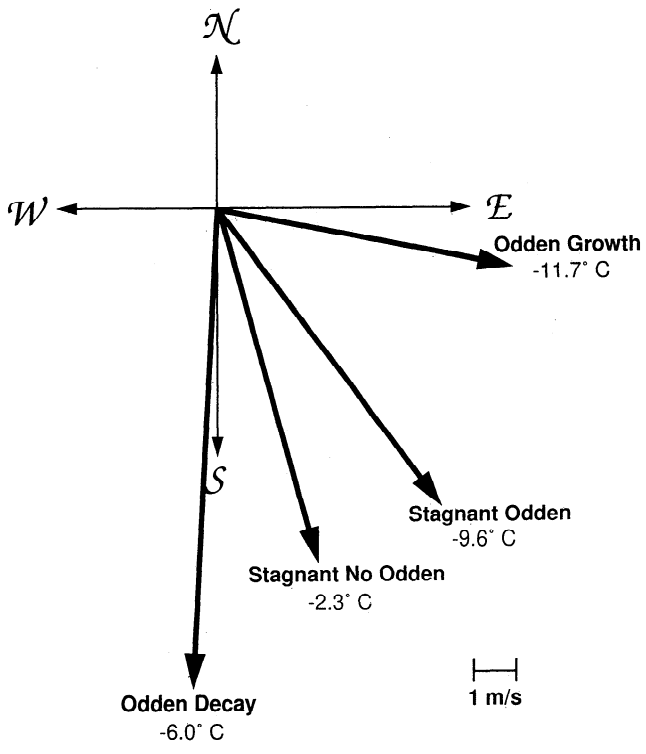

Figure 4. Results of meteorological analysis showing mean wind speed, direction, and temperature for Odden growth, Odden decay, stagnant Odden, and stagnant no-Odden cases.

growth rates was found to be -11.7°C, nearly 5°C colder than the -7.0°C wintertime average for this region. To maintain the Odden requires an average temperature of -9.6°C. The average temperature during Odden ice decay was found to be -6.0°C, only 1°C above the wintertime average. Under relatively warm conditions, as would be expected, no Odden forms at all, and this is supported by the average temperature of -2.3°C for the stagnant no-Odden case.

Wind speed and direction also appear to play a role during the Odden ice pack formation and decay, which influences the surface heat flux, the ice drift, and upper ocean currents. As shown in Figure 4, Odden formation occurs when winds are moderate and out of the west, bringing very cold air from the Greenland Ice Sheet. These off-ice wind conditions will generate downwelling in the surface layers at the ice edge [*O.M. Johannessen et al.*, 1983; 1992; *J.A. Johannessen et al.*, 1987]. Because the temperature of the upper 200 m in the Greenland Sea is generally warmer than the surface layers, Odden formation can only occur after the surface waters are sufficiently cooled. This may explain why Odden events are only associated with very cold wind events.

At the other extreme, Odden decay is associated with very high winds, 12.4 m s^{-1} on average, from the north, and air temperatures of -6.0°C. It is theorized that decay occurs through the combination of increased melting and mechanical destruction at the ice edge. The northerly and northeasterly winds transport both ice and water to the southwest; however, because the ice is rougher, it moves faster than the underlying water. At the southern edge of the Odden the ice moves out into the relatively warm open Greenland Sea and rapidly melts. Ice in the northern portion of the Odden also moves into the open water, in this case the Nordbukta, and melts. Also at the northern edge, the strong northerly winds of 12 m s^{-1} will generate fully developed wave conditions that will continuously hammer the northerly portions of the Odden. The impact of these waves will break up and flood the young ice types of the Odden, which will greatly accelerate the melting of the ice. Plates 2 and 3 show that the Odden does not drift significantly to the southwest under these conditions. This results from the strong horizontal temperature gradients in the region and the 50-km resolution of the passive microwave imagery. The ice may melt very quickly (within one pixel or less) as it is pushed over warmer waters to the southwest; a similar process is also observed in the Bering Sea [*Muench*, 1990]. The stagnant Odden and stagnant no-Odden cases are not noticeably different in wind speed or direction from the wintertime average wind speed of 9.2 m s^{-1} and northwesterly wind direction of 317°. The similarity of the two stagnant cases to the winter climatology suggests that wind speed plays a secondary role to temperature during ice formation, maintenance, and decay.

In addition to the statistics calculated for each of the four Odden cases, various pairs of time series were analyzed to determine if there was any delay between the meteorological forcing and the ice formation. The strongest relationships were found between the temperature and growth rate time series. Plate 3 shows a particularly active winter season (November 1981 to April 1982) in which numerous growth and decay events occurred. Figure 5 shows the Odden growth rate along with the meteorological data for the same time period. The growth rate was calculated by first interpolating the SMMR-derived Odden area to twice-daily sampling (to correspond to the temperature sampling rate), then taking the difference between every two successive points and finally smoothing the data with a seven point running boxcar filter. The temperature time series has been averaged with a five point running boxcar filter. Visually, Figure 5 shows that the growth rate appears somewhat anticorrelated with air temperature and in phase as physically expected. In this case, however, the correlation coefficient was only R=-0.29, which is nonetheless statistically significant at the 0.99 level [*Bickel and Doksum*, 1977]. The physical relationship is seen in the individual cases, such as in the example shown in Figure 6 for the 60-day time period from January 21 through March 20, 1979. The correlation coefficient for this particular time series was -0.68, which is also statistically significant at the 0.99 level. While similar time periods for other years showed weaker correlation than the 1979 period, they still showed an inverse relationship between ice growth and air temperature. The conclusion from this analysis was that while some mixed layer preconditioning appears to be required for Odden growth, it also appears that ice growth responds almost immediately to low temperature forcing and ice decay to warm temperature forcing.

The wind speed and direction also influence ice growth or decay; moderate winds from the west and northwest yield ice growth while strong winds from the north and northeast yield ice decay, as shown in Figure 4. Cold westerly winds of 7-8 m s^{-1}, with typical temperatures of –11°-12°C, are sufficient to cause significant ice formation. Although only a few degrees warmer, the strong winds from the north and northeast do not generate ice but actually diminish the Odden through the processes described earlier. Unlike the immediate response in growth rate to changes in temperature, however, there does not appear to be an immediate response in ice growth rate to changes in wind speed. Therefore wind speed is believed to be a necessary and important forcing parameter, but air temperature is the dominant atmospheric forcing parameter.

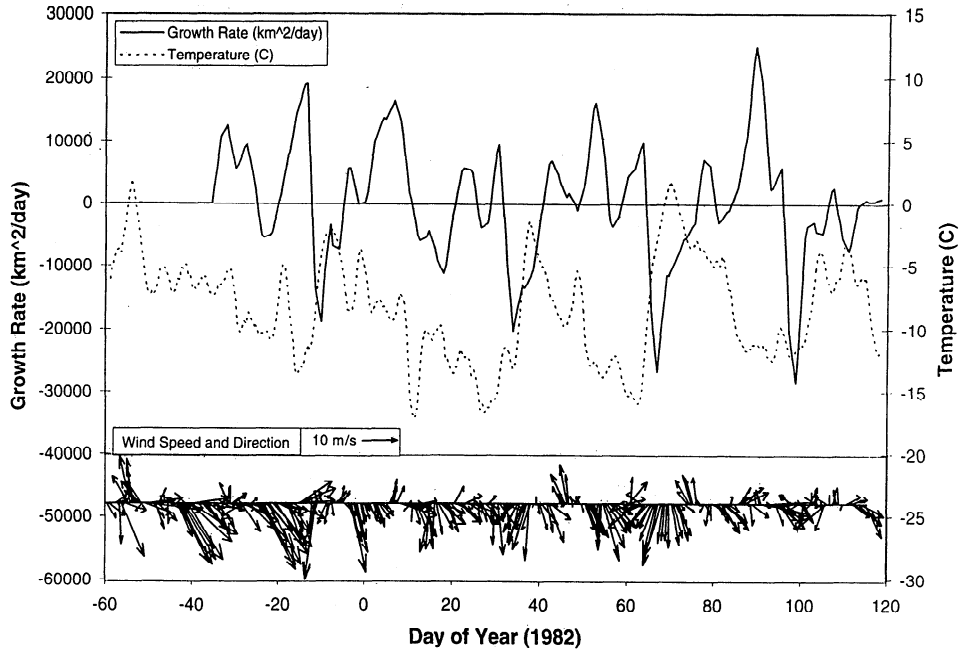

Figure 5. Winter 1981-1982 time series showing SMMR-derived Odden ice growth rates with corresponding buoy-derived meteorological parameters. Notice the high inverse correlation between growth rate and temperature.

This analysis shows that meteorological conditions play a definite role in controlling ice formation in the Odden region. Some preconditioned cooling of the ocean surface water is certainly required to allow the ice to form, but it is not clear from the available data what that preconditioning may be. It appears that typical winter conditions in the Greenland Sea provide adequate preconditioning for the Odden to form much of the time and that the actual ice formation is a short-term response to meteorological forcing, primarily moderate cold winds form the northwest. Nonetheless, the overlap of the temperature distributions from each of the four cases considered indicates that ice growth does not always follow from cold temperatures and weak winds, so preconditioning of the ocean surface layer must have some effect. Of the meteorological parameters, temperature is the most significant forcing parameter; wind speed followed by wind direction are of slightly lower, but still significant, importance.

One goal of this investigation is to determine a temperature threshold below which significant Odden growth occurs. To this end, the distribution of temperatures associated with significant ice growth events was compared with the distribution of temperatures over the entire winter season. The first step was to determine whether these classes were, in fact, statistically different. A statistical t test on the confidence intervals of the

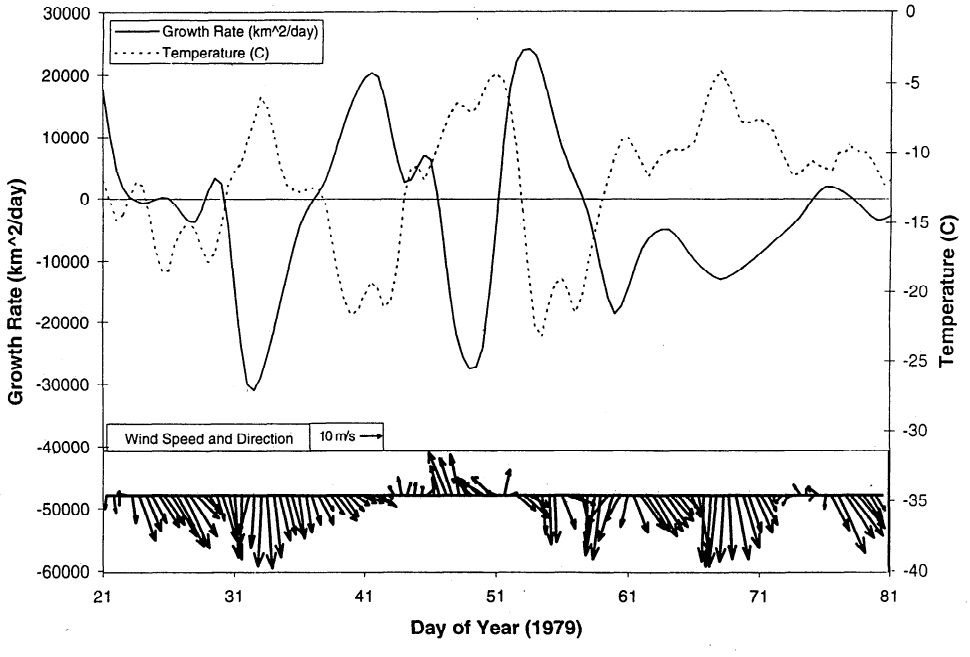

Figure 6. Sixty-day time series showing SMMR-derived Odden ice growth rate with corresponding buoy-derived meteorological parameters during the period January 21 to March 20, 1979.

two distributions showed that the two distributions were statistically different at greater than the 0.99 level. Next, a standard statistical classification for normal distributions was performed for the two temperature classes to determine the optimum threshold temperature to separate the two classes. The classification of the two classes of temperature values (Odden growth versus wintertime average) resulted in a temperature threshold of –8.7°C, below which substantial ice begins to form. This threshold can be used to classify periods of time into growth versus nongrowth types (decay, stagnant Odden, stagnant no-Odden, and remaining periods). The classification statistics are summarized in Table 2a. A similar temperature threshold strategy was used to separate periods of stagnant Odden maintenance from periods of Odden ice decay. The results showed that the two distributions were also statistically different at greater than the 0.99 level and that the optimum threshold temperature was –8.0°C with classification statistics given in Table 2b. The relatively large probabilities of error (misclassification) indicate that surface air temperature is not the only parameter responsible for ice formation. It should also be noted that it is difficult to separate out cause and effect in this case since no time lags between the two time series could be found. The presence of ice may, in fact, have been the cause of the lower air temperatures. Nonetheless, the association of lower air temperatures with high ice formation rates appears to be genuine. The following section considers the degree to which these relationships are seen in the interannual variability of the Odden.

4. Interannual Odden Variability

In addition to the strong intra-annual variability discussed in the previous section, the Odden displays strong interannual variability of spatial coverage and temporal characteristics (see Figures 3a and 3b). For some years the Odden was quite large, covering nearly 300,000 km^2 of the Greenland Sea, while for other years it was practically nonexistent. Additionally, for some years the Odden advanced and remained nearly constant through the winter, while for other years it repeatedly advanced and retreated. Figure 7 summarizes both the behavior of the Odden obtained from the 16-year satellite record and the meteorological conditions from each winter.

4.1. Odden Ice Area Interannual Variability

Figures 7a and 7b show the maximum Odden area and the mean Odden area for the period of record; both parameters exhibit similar behavior. For the first four winters, 1978-1979 through 1981-1982, there was a strong Odden, with the maximum area covered being ~200,000 km^2, and the mean area was about 80,000 km^2. For the winters of 1982-1983 and 1983-1984 the Odden was very weak; it returned in 1984-1985 and encompassed the greatest area in 1985-1986. Inspection of the time series in Figures 3a and 3b shows that for 1983-1984 the Odden essentially did not occur and that in 1984-1985 the Odden returned in January, later than normal. This indicates that the period of weak Odden occurrence spanned nearly three winters, with a minimum for the winter of 1983-1984.

Table 2a. Temperature Classification Statistics

	Probability of Correct Classification	Probability of Incorrect Classification
Odden growth	0.61	0.39
Wintertime average	0.70	0.30

Temperature threshold is 8.7°C.

Table 2b. Temperature Classification Statistics

	Probability of Correct Classification	Probability of Incorrect Classification
Stagnant Odden	0.63	0.37
Odden decay	0.67	0.33

Temperature threshold is –8.0°C.

The four winters from 1984-1985 through 1988-1989 had the strongest Odden conditions in the entire record. Both the maximum area and the mean area attained values near 300,000 km^2 and 125,000 km^2, respectively. Despite the apparent similarity of these years, the time series in Figures 3a and 3b show that each year is different. The time of maximum coverage varies from year to year, as does the time of initial Odden occurrence, and subsequent temporal characteristics are quite different. For the three winters of 1989-1990, 1990-1991, and 1991-1992 the Odden occurred at a consistently low level with a maximum extent of 150,000 km^2 and mean area of about 50,000 km^2. Figures 3a and 3b show that the Odden frequently disappeared during these winters. The Odden for the winters of 1992-1993 and 1993-1994 behaved similarly to that observed in 1982-1983 and 1983-1984, a weak occurrence followed by a nearly complete absence. One might speculate that this suggests two interesting phenomena: first, there is a decadal periodicity in weak Odden years; second, the unidentified mechanisms that generate a weak Odden persist for 2 or 3 years. Clearly, a much longer time series would be required to conduct a meaningful analysis on periodicity at this timescale.

While the Odden maximum area and the average area covered are important factors in the heat and salt budgets of the Greenland Sea, the fluctuations in the Odden may be more important. Odden advances across the Greenland Sea may inject pulses of salt through the brine rejection that takes place as the sea water freezes [*Wadhams et al.*, 1996]. To evaluate this effect for each year, we computed the accumulated ice growth (AIG) and the root mean square (RMS) difference between the actual record and a smoothed record. The AIG is the cumulative increase in ice-covered area through a given winter, which ignores periods of Odden decay, and is shown in Figure 7c. To compute the RMS difference, each times series was smoothed with a 31-day boxcar filter and then this was subtracted from the original time series. Figure 7d shows the RMS difference between the two time series for each year. When compared to the AIG, the RMS difference shows much less variation from year to year. For years with weak to strong Odden events, the RMS difference ranged from 18,000 to 30,000 km^2 with most of the values near 20,000 km^2.

The AIG shows that the amount of Odden ice growth in a given year is always much greater than either the maximum area or the mean area. A comparison of the AIG to the maximum area shows that the ice produced in the Greenland Sea is 2-3 times greater than the maximum area covered. This is not surprising since ice in this region is constantly melting because of warm ocean temperatures, and the ice is maintained by constant ice growth. When compared to the mean area, the ice production is

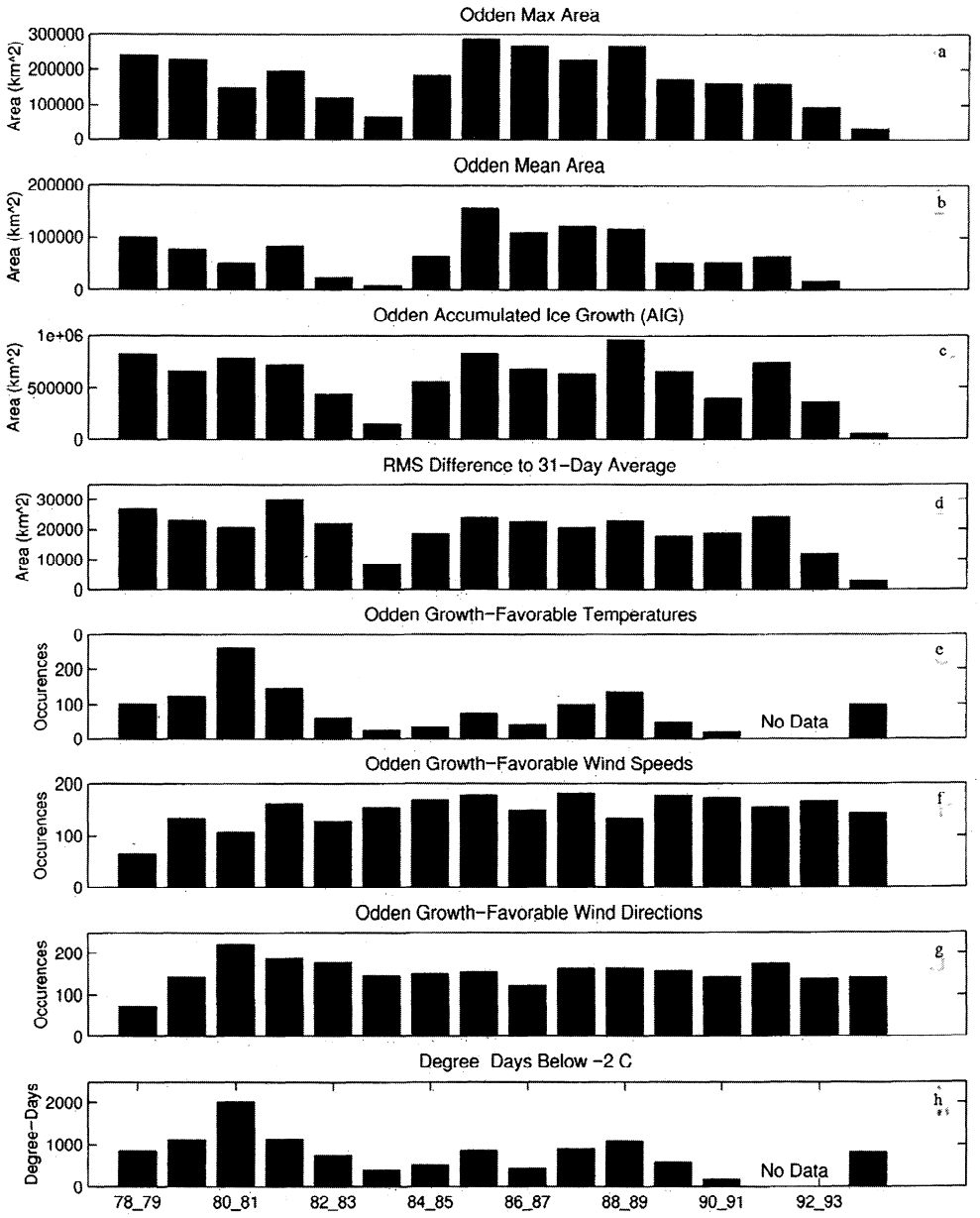

Figure 7. Annual statistics for (a) Odden ice maximum area, (b) Odden ice mean area, (c) accumulated ice growth, (d) RMS difference to 31-day average, (e) number of occurrences of Odden growth-favorable temperatures, (f) number of occurrences of Odden growth-favorable wind speeds, (g) number of occurrences of Odden growth-favorable wind directions, and (h) number of degree days below -2°C.

3-5 times greater. The ice production is near zero for winters with little Odden activity, 1983-1984, 1993-1994, and 1994-1995. For winters with low Odden activity, 1982-1983 and 1992-1993, the ice production was still surprisingly large, about 400,000 km^2. The two periods of the record with strong Odden events, 1978-1979 through 1981-1982, and 1984-1985 through 1988-1989 had AIG values of 600,000 to 1,000,000 km^2, and the latter value occurred in the winter of 1988-1989. If the Odden plays a significant role in generating deep convection by destabilizing the water column through brine rejection, then the yearly total ice production (AIG) is a much more important factor than the maximum or average ice-covered area. The relationship between Odden events and deep convection is discussed in greater detail in section 5. Section 4.2 discusses the long-term trends in the meteorological conditions.

4.2. Odden Interannual Variability and Meteorological Conditions

Figure 7e-7g show the number of growth-favorable temperatures, wind speeds, and wind directions that occurred during the winters of the study years, and Figure 7h shows the number of degree days below -2°C for each winter. Figure 7e shows the number of occurrences during each winter of temperatures below -9.5°C, the estimated temperature threshold for significant Odden ice formation. Buoy-derived atmospheric

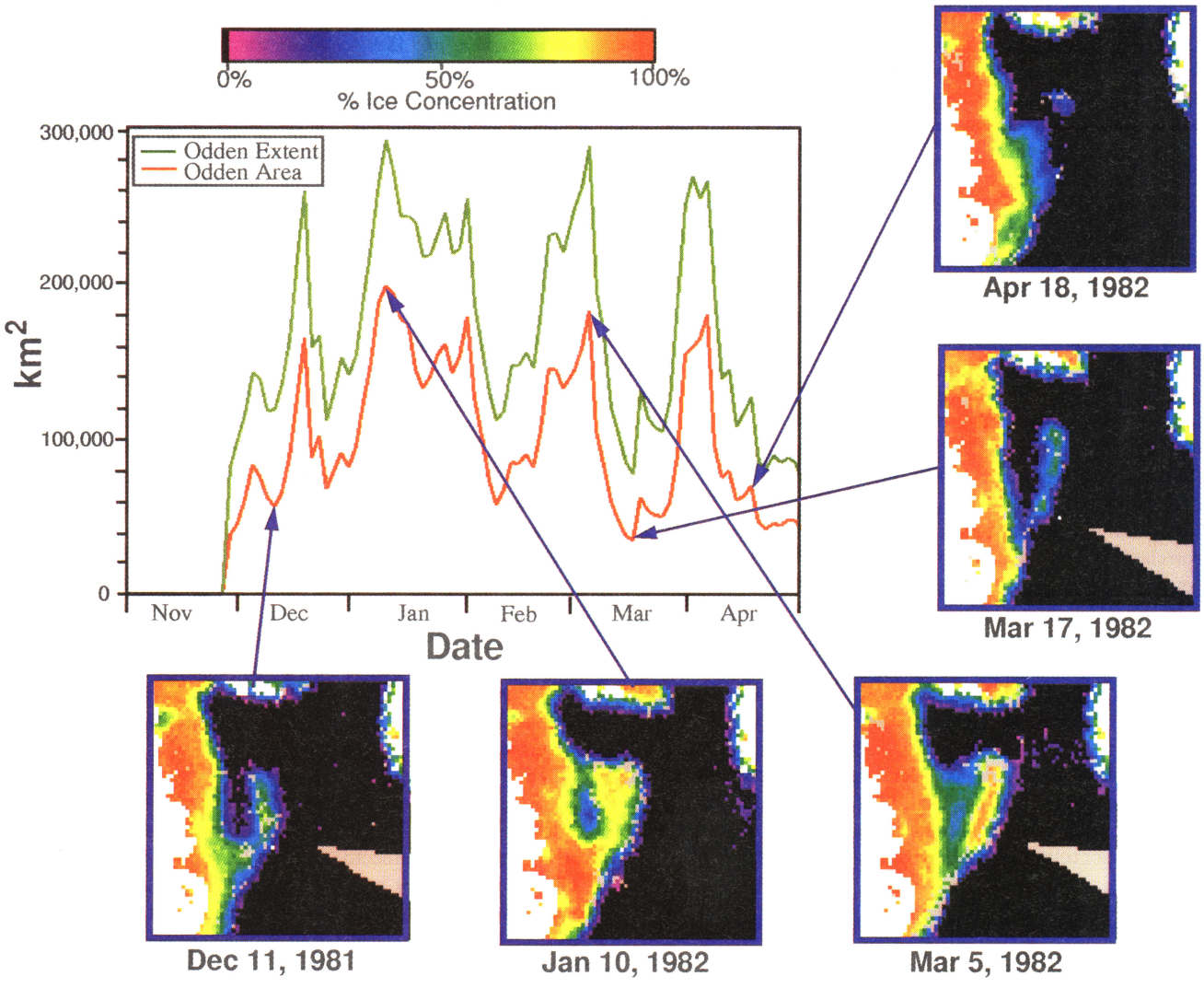

Plate 3. Time series of Odden area and extent for the 1981-1982 winter season. Extreme variability in the Odden is illustrated by the pullouts of SMMR-derived ice concentration maps at specific points in the time series.

temperatures for the Odden region were not available for January through April 1991 and for the winters of 1991-1992 and 1992-1993. Figure 7f shows the number of occurrences of Odden growth-favorable wind speeds from 4.7 to 10.7 m s^{-1} (mean ±3 m s^{-1}). Figure 7g shows the number of occurrences of Odden growth-favorable wind directions in the range 56°-146° (mean ± 45°) clockwise off north.

In general, Figure 7 shows that the relationship between the favorable atmospheric conditions and the Odden is weak at best. The temperature records in figures 7e and 7h suggest that there is a weak link between the Odden and the temperature. The two periods of strong Odden activity, 1978-1979 through 1981-1982 and 1984-1985 through 1988-1989, had the largest number of temperature-favorable conditions and the greatest number of degree days. The first period had the coldest temperatures but somewhat less favorable wind conditions, while the second period was warmer, an effect that was countered by more occurrences of favorable wind conditions. This lack of correlation with the entire meteorological data set shows that the temperature and wind conditions that we derived for Odden growth are necessary but not sufficient. Odden formation is a complex process that involves not only the atmosphere but also the highly variable Greenland and Norwegian Seas. Unfortunately, oceanographic data sets comparable to the meteorological data sets used in this analysis do not exist, as will be discussed in section 5.

4.3. Odden and Global Atmospheric Circulation Patterns

The great annual variation of the Odden, particularly the periods of minimum Odden ice extent that appear to be related to relatively warmer winters, suggests a possible link to changes in the global atmospheric circulation patterns. To determine if there are any significant relationships, we examined two of the most dominant global circulation indices, the North Atlantic Oscillation (NAO) and the El Niño-Southern Oscillation (ENSO) indices. *Hurrell* [1995] showed that the winter atmospheric circulation patterns in the North Atlantic region that are associated with positive values of the NAO index consist of anomalously low pressure across the Arctic and higher than normal pressure south of 55° N. This pattern produces stronger

than normal westerlies into Europe, with an anomalous northerly flow across western Greenland. The correlation between the NAO index and the annual maximum area covered by Odden ice was R= 0.42, which is not statistically significant at the 0.95 level. With the Odden conditions lagging by 1 year, the correlation increased to 0.59, which is statistically significant at the 0.95 level. With a lag of 2 years, the correlation decreased to 0.36, which is again not statistically significant at the 0.95 level. While not extraordinarily high, the correlation at a 1-year lag is statistically significant and suggests that the previous winter may play a role in determining the maximum Odden ice conditions, perhaps by modifying the upper ocean conditions in the Greenland Sea.

Gloersen [1995] and *Gloersen et al.* [1996] investigated the relationship between ENSO events as characterized by the Southern Oscillation Index (SOI) and global sea ice conditions determined from the SMMR period, 1978 through 1987. These studies found significant correlations between SOI and the sea ice cover, including the Greenland Sea ice cover. Using the combined SMMR and SSM/I data sets, we find surprisingly low correlations of Odden maximum ice cover and SOI. A correlation study similar to the one described above for the NAO used the monthly SOI values averaged to yield quarterly values. The lag time between the Odden and the SOI ranged from zero to four quarters, or 1 year. For no lag the correlation was R=0.33; for a lag of 3, 6, and 9 months, the correlations were 0.42, 0.41, and 0.44, respectively. The correlation then dropped to 0.37 for a 1-year lag. Beyond a lag of 1 year, there was no appreciable correlation. None of these correlation coefficients are statistically significant at the 0.95 level. These low correlations with atmospheric circulation indices further indicate that the ocean plays a major role in controlling Odden formation.

5. Discussion: Relation of Odden Events to Deep Ocean Convection

The Odden is clearly not solely controlled by atmospheric conditions; it is also strongly influenced by the oceanographic conditions and processes along the marginal ice zone in the Greenland Sea, which are characterized by the complex interactions of transient upper ocean features and processes with the mean background circulation. Upper ocean eddies, jets, and zones of upwelling and downwelling are frequently observed along the ice edge [*J.A. Johannessen et al.*, 1987; *O.M. Johannessen et al.*, 1994]. These transient features effectively modify the mean conditions through changes in the mixed layer depth and in the transport of heat, salt, and freshwater, both vertically and horizontally. It is not yet possible, however, to quantify the relative contribution of these transient processes and of the Odden to deep water formation. Long-term oceanographic data sets of sufficient temporal and spatial resolution necessary to characterize the effects of the extremely energetic mesoscale, and the smaller processes on the much less energetic general circulation in the Greenland Sea simply do not exist.

Because it is believed that deep convection is closely linked to the timing and location of the Odden, improving our understanding of deep water formation may result from increasing our understanding of the Odden and its response to the various forcing mechanisms. The Odden may play a key role in deep water formation or may just be an indicator of deep convection or the absence thereof. *Killworth* [1979], *Paluszkiewicz et al.* [1994], *Schott et al.* [1993], and *Visbeck et al.* [1995, 1996] show that the deep ocean convection in the Greenland Sea requires extreme cooling and enhanced salinity of the upper ocean that could be the result of brine rejection by Odden ice formation. The deep convection that renews the North Atlantic Deep Water and plays a key part in the thermohaline circulation of the world's oceans is believed to occur in the Greenland Sea in the open water area between the Odden and Greenland.

Definitive long-term records of deep convection are scarce. *Alekseev et al.* [1994] analyzed CTD data from the Odden area for the period 1950-1993 for evidence of deep convection. In the early portion of the record, 1950-1976, the coverage is sparse; however, in the latter portion, there are 150 CTD casts or more for each year. Decreases in the average potential temperature for depths >1000 m are interpreted to indicate the occurrence of deep convection. For the period analyzed in this study, convection occurred in 1981, 1984, 1986, 1988, and 1989. *Alekseev et al.* [1994] also show that temperature and salinity conditions in the upper few hundred meters are strongly related to the occurrence of deep convection. For the years that convection occurred, the upper layer temperature and salinity are ~1°C warmer and 0.02 psu more saline than those for years with no convection. *Østerhus et al.* [1996] report on the long-term oceanographic

Table 3. Deep Water Convection Versus Odden Occurrences

Year	Convection	Odden Maximum Area, km^2	Odden Comment
1978-1979	yes	243,025	strong
1979-1980	no	230,431	strong
1980-1981	yes	151,550	moderate
1981-1982	no	198,194	strong, highly variable
1982-1983	no	122,850	weak, disappeared early
1983-1984	yes	67,625	very weak
1984-1985	no	186,350	moderate, returned late
1985-1986	yes	289,181	strong, stagnant
1986-1987	no	286,300	strong, stagnant
1987-1988	yes	227,369	strong,
1988-1989	yes	268,281	strong, variable late in season
1989-1990	no	194,356	strong to moderate
1990-1991	no	164,075	moderate
1991-1992	no	163,456	moderate
1992-1993	no	97,351	weak, disappeared early
1993-1994	no	33,056	none

observations from the ocean weather ship *Mike* located in the southeast portion of the Norwegian Sea, in the region where North Atlantic water flows into the GIN Sea region. Measurements in the central Greenland Sea at 2000 m show a continuous warming since 1980. They interpret the temperature trends to indicate a cessation of Greenland Sea deep water since 1980.

Table 3 summarizes the results of *Alekseev et al.* [1994] and *Østerhus et al.* [1996] and the annual Odden conditions. The relation between the satellite passive microwave Odden observations and the indirect observations of the occurrence of deep convection is not clear. In 1980-1981 and 1983-1984, there was evidence of deep convection, and the Odden was weak or nonexistent. However, in 1985-1986, 1987-1988, and 1988-1989, deep convection again was evident, but the Odden was strong. For the 4-year period from 1989-1990 to 1992-1993, there is no evidence of deep convection, and the Odden was generally weak. Therefore the Odden or any of the Odden characteristics that we have derived may not be directly related to deep convection. While we can determine the necessary meteorological conditions during Odden growth and decay, the interannual variations of the Odden area indicate that while the meteorological forcing plays a dominant role, oceanographic conditions are also important in determining Odden conditions. The meteorological record shows that many years have nearly similar occurrences of Odden favorable conditions, yet the Odden for those years are quite different. The apparent 10-year cycle of 3-year minimum Odden events may be related to varying oceanographic events and the episodic occurrence of deep convection alternating between the Greenland Sea and the Labrador Sea. Current theories of deep convection require brine rejection by Odden ice formation to destabilize the upper ocean. However, the only 17-year record of deep convection in the Greenland Sea, which has been inferred from CTD records in the area, shows no direct relationship to Odden events.

6. Summary

Typically, the Odden forms in December of each year and disappears in middle to late April. It encompasses up to 300,000 km^2 and extends to 5°E at 75°N at its maximum extent and undergoes rapid advances and retreats throughout the winter. To better understand the rapid formation and decay of the Odden, this study utilized satellite passive microwave data from the SMMR and the SSM/I satellite sensors, aircraft SAR data, in situ buoy data, and modeled atmospheric pressure and temperature fields. The comparisons between the ice edges derived from the SAR and SMMR observations are in good agreement. The SAR-derived sea ice concentrations agreed to within 10%, of the SMMR-derived total ice concentration.

An analysis of the SMMR- and SSM/I-derived ice area and extent time series with meteorological data from the International Arctic Buoy Program showed that the Odden is a result of new ice formation rather than the advection of ice away from the main pack. The analysis also determined the meteorological conditions that are associated with Odden growth, maintenance, and decay. Air temperatures below –8.7°C and moderate winds from the northwest are associated with significant ice growth. The ice formation appears to respond almost immediately to cold temperatures, and no significant delay is seen between the onset of cold temperatures and the increase in ice formation rate. Odden decay occurs during warmer conditions (an average of ~ 6°C) and with strong winds out of the north. A temperature of ~ –8.0°C is the threshold between maintaining the Odden ice formation and Odden ice decay. In all cases, air temperature alone cannot be used to effectively classify ice growth regime indicating that other meteorological and oceanographic parameters play a significant role in ice formation.

The annual variability of the Odden is large, with Odden ice-covered area ranging from 0 to 300,000 km^2. The 17-year record suggests a possible 10-year cycle in the Odden minimums, although clearly a much longer time series would be required to validate this interpretation. The accumulated ice growth (AIG), which is the total amount of ice formed in each year, shows even greater variability, ranging from near 0 to 1,000,000 km^2 and is much greater than the maximum ice-covered area. The AIG is probably more important than the maximum ice extent in the salt budget of the Greenland Sea because of the brine rejection that occurs during the freezing process.

The meteorological conditions derived from the 17-year record for Odden growth, summarized in Table 1, are found to be necessary but not sufficient to determine Odden variations. This strongly suggests that the oceanographic conditions of the Greenland Sea play a key role, as the formation and decay of the Odden results from the complex interaction of the atmosphere, ice, and ocean in the Greenland Sea region. Because of the lack of long-term synoptic oceanographic data sets analogous to the meteorological and sea ice data sets, it is difficult to determine the causes of the Odden and its variations. The limited oceanographic record shows little relationship between the Odden and deep convection in the Greenland Sea. We have shown, however, that meteorological forcing plays an important, if not dominant, role in the formation and variability of the Odden.

Acknowledgments. The ERIM International portion of this analysis was supported by Office of Naval Research (ONR) contract N00014-81-C-0295. The ONR Technical Monitor was Charles A. Luther. The USGS participation was supported by the Global Change Program (Harry Lins, Water Resources Division Global Change Research Coordinator). The NASA Goddard analysis was supported by the NASA Nimbus Project Office. The Nansen Environmental Remote Sensing Center contributions were also performed under ONR sponsorship (Tom Curtin, Technical Monitor). The authors would also like to acknowledge the contributions of Jeff Rash for the meteorological analysis. The authors offer a grateful thanks to William Campbell (1930-1992) for his ideas which contributed to the early stages of this work.

References

Aagaard, K., and E. C. Carmack, The role of sea ice and other freshwater in the Arctic circulation., *J. Geophys. Res., 94*(C10), 14,485-14,498, 1989.

Alekseev, G. V., V. V. Ivanov, and A. A. Korablev, Interannual variability of the thermohaline structure in the convective gyre of the Greenland Sea, in *The Polar Oceans and Their Role in Shaping the Global Environment: The Nansen Centennial Volume, Geophys. Monogr. Ser.*, vol. 85, edited by O. M. Johannessen, R. D. Muench, and J. E. Overland, pp. 485-496, AGU, Washington D.C., 1994.

Bickel, P. J., and K. A. Doksum, *Mathematical Statistics: Basic Ideas and Selected Topics*, Holden-Day, Merrifield, VA 1977.

Bourke, R. H., R. G. Paquette, and R. F. Blythe, The Jan Mayen Current of the Greenland Sea, *J. Geophys. Res., 97*(C5), 7241-7250, 1992.

Campbell, W. J., P. Gloersen, E. G. Josberger, O. M. Johannessen, P. S. Guest, N. Mognard, R. Shuchman, B. A. Burns, N. Lannelongue, and K. L. Davidson, Variations of mesoscale and large-scale sea ice morphology in the 1984 Marginal Ice Zone Experiment as observed by microwave remote sensing, *J. Geophys. Res., 92*(C7), 6805-6824, 1987.

Campbell, W. J., P. Gloersen, and H. J. Zwally, Short- and long-term

temporal behavior of polar sea ice covers from satellite passive-microwave observations, in *The Polar Oceans and Their Role in Shaping the Global Environment: The Nansen Centennial Volume*, *Geophys. Monogr. Ser.*, vol. 85, edited by O. M. Johannessen, R. D. Muench, and J. E. Overland, pp. 505-520, AGU, Washington, D.C. ,1994.

Cavalieri, D. J., P. Gloersen, and W. J. Campbell, Determination of sea ice parameters with the Nimbus 7 SMMR, *J. Geophys. Res., 89*(D4), 5355-5369, 1984.

Colony, R. I., and I. Rigor, International Arctic Buoy Program data report: 1 January 1993-31 December 1993, *Appl. Phys. Lab. Tech. Memo. TM 04-95*, Appl. Phys. Lab., Univ. of Wash., Seattle, 1995.

Dickson, R. R., J. Meincke, S.-A. Malmberg, and A. J. Lee, The "great salinity anomaly" in the northern North Atlantic 1968-1982, *Prog. Oceanogr., 20*, 103-151, 1988.

Eppler, D. T., et al., Passive microwave signatures of sea ice, in *Microwave Remote Sensing of Sea Ice*, *Geophys. Monogr. Ser.*, vol. 68, edited by F. D. Carsey, pp. 47-71, AGU, Washington, D.C., 1992.

Gloersen, P., Modulation of hemispheric sea-ice cover by ENSO events, *Nature, 373*, 503-506, 1995.

Gloersen, P., and F. T. Barath, A scanning multichannel microwave radiometer for Nimbus G and Seasat, *IEEE J. Oceanic Eng., OE-2*, 172-178, 1977.

Gloersen, P., and D. J. Cavalieri, Reduction of weather effects in the calculation of sea ice concentration from microwave radiances, *J. Geophys. Res., 91*(C3), 3913-3919, 1986.

Gloersen, P., et al., A summary of results from the first Nimbus 7 SMMR observations, *J. Geophys. Res., 89*(D4), 5335-5344, 1984.

Gloersen, P., W. J. Campbell, D. J. Cavalieri, J. C. Comiso, C. L. Parkinson, and H. J. Zwally, Arctic and Antarctic sea ice, 1978-1987: Satellite passive-microwave observations and analysis, *NASA Spec. Publ. SP, NASA SP-511*, 15-42, Washington, D.C., 1992.

Gloersen, P., Y. Jun, and E. Mollo-Christensen, Oscillatory behavior in Arctic sea ice concentrations, *J. Geophys. Res., 101*(C3), 6641-6650, 1996.

Grenfell, T. C., D. J. Cavalieri, J. C. Comiso, M. R. Drinkwater, R. G. Onstott, I. Rubinstein, K. Steffen, and D. P. Winebrenner, Considerations for microwave remote sensing of thin sea ice, in *Microwave Remote Sensing of Sea Ice*, *Geophys. Monogr. Ser.*, vol. 68, edited by F. D. Carsey, pp. 291-301, AGU, Washington, D.C., 1992.

Hollinger, J., DMSP special sensor microwave/imager calibration/validation final report, vol. I, report, Nav. Res. Lab., Washington, D.C., 1989.

Hopkins, T. S., The GIN Sea: Review of physical oceanography and literature from 1972, *Rep. SACLANT-CEN SR-124*, SACLANT Undersea Res. Cent., La Spezia, Italy, 1988.

Hurrell, J. W., Decadal trends in the North Atlantic Oscillation: Regional temperatures and precipitation, *Science, 269*, 676-679, 1995.

Johannessen, J. A., et al., Mesoscale eddies in the Fram Strait marginal ice zone during the 1983 and 1984 Marginal Ice Zone Experiments, *J. Geophys. Res. 92*(C7), 6754-6772, 1987.

Johannessen, O. M., J. A. Johannessen, J. Morison, B. A. Farrelly, and E. A. S. Svendsen, Oceanographic conditions in the marginal ice zone north of Svalbard in early fall 1979 with an emphasis on mesoscale processes, *J. Geophys. Res., 88*(C5), 2755-2769, 1983.

Johannessen, O. M., W. J. Campbell, R. Shuchman, S. Sandven, P. Gloersen, J. A. Johannessen, E. G. Josberger, and P. M. Haugan, Microwave study programs of air-ice-ocean interactive processes in the seasonal ice zone of the Greenland and Barents Seas, in *Microwave Remote Sensing of Sea Ice*, *Geophys. Monogr. Ser.*, vol. 68, edited by F.D. Carsey, pp. 261-289, Washington, D.C., 1992.

Johannessen, O. M., S. Sandven, W. P. Budgell, J. A. Johannessen, and R. A. Shuchman, Observation and simulation of ice tongues and vortex pairs in the marginal ice zone, in *The Polar Oceans and Their Role in Shaping the Global Environment: The Nansen Centennial Volume, Geophys. Monogr. Ser.*, vol. 85, edited by O. M. Johannessen, R. D. Muench, and J. E. Overland, pp. 109-136, AGU, Washington, D.C., 1994.

Killworth, P. D., On chimney formations in the ocean, *J. Phys. Oceanogr., 9*, 531-554, 1979.

Mardia, K. V., *Statistics of Directional Data*, Academic, San Diego, Calif. 1972.

MIZEX'87 Group, MIZEX East 1987: Winter marginal ice zone program in the Fram Strait and Greenland Sea, *Eos Trans. AGU, 70*(17), 545, 548-549, 554-555, 1989.

Muench, R. D., Mesoscale phenomena in the polar oceans, in *Polar Oceanography, Part A: Physical Science*, edited by W. O. Smith Jr., pp. 223-287, Academic, San Diego, Calif. 1990.

National Snow and Ice Data Center (NSIDC), DMSP SSM/I brightness temperature and sea ice concentration grids for the polar regions on CD-ROM: User's guide, *Nat. Snow and Ice Data Cent. Spec. Rep. 1*, Boulder, Colo., 1992.

National Snow and Ice Data Center (NSIDC), Nimbus 7 SMMR polar radiances and Arctic and Antarctic sea ice concentrations on CD-ROM: User's guide, *Nat. Snow and Ice Data Cent. Spec.* Ver. 3, Boulder, Colo., 1994.

Østerhus, S., T. Gammelsrød, and R. Hogstad, Ocean weather ship station M (66°N, 2°E): The longest homogeneous time series from the deep ocean, *Int. World Ocean Circ. Exp. (WOCE) Newsl., 24*, 31-33, 1996.

Paluszkiewicz, T., R. W. Garwood Jr., and D. W. Denbo, Deep convective plumes in the ocean, *Oceanography*, 7(2), 37-44, 1994.

Parkinson, C. L., J. C. Comiso, H. J. Zwally, D. J. Cavalieri, P. Gloersen, and W. J. Campbell, Arctic Sea Ice, 1973-1976: Satellite passive-microwave observations, *NASA Spec. Publ. SP-489*, pp. 41-108, 1987.

Schlosser, P., G. Bönisch, M. Rhein, and R. Bayer, Reduction of deep water formation in the Greenland Sea during the 1980s: Evidence from tracer data, *Science, 251*, 1054-1056, 1991.

Schott, F., M. Visbeck, and J. Fischer, Observations of vertical currents and convection in the central Greenland Sea during the winter of 1988-1989, J. *Geophys. Res., 98*(C8), 14,401-14,421, 1993.

Shuchman, R. A., and R. G. Onstott, Remote sensing of the polar oceans, in *Polar Oceanography*, part A, *Physical Science*, edited by W. O. Smith Jr., pp. 123-171, Academic, San Diego, Calif., 1990.

Shuchman, R. A., L. L. Sutherland, B. A. Burns, and E. D. Leavitt, MIZEX 1987 SAR data summary, *ERIM Inf. Rep. 154600-34-T*, Off. of Nav. Res., Arlington, Va., 1988.

Shuchman, R. A., C. C. Wackerman, A. L. Maffett, R. G. Onstott, and L. L. Sutherland, The discrimination of sea ice types using SAR backscatter statistics, in *IGARSS '89, IEEE Publ. 89CH2768-0*, pp. 381-386, IEEE Press, Piscataway, N.J., 1989.

Toudal, L., Multisensor observations of winter sea ice in the Greenland Sea, in Oceanic Remote Sensing and Sea Ice Monitoring Symposium, edited by J.A. Johannessen and T.H. Guymer, *Proc. SPIE Int. Soc. Opt. Eng., 2319*, pp. 126-133, 1994.

Tucker, W. B., III, T. C. Grenfell, R. G. Onstott, D. K. Perovich, A. J. Gow, R. A. Shuchman, and L. L. Sutherland, Microwave and physical properties of sea ice in the winter marginal ice zone, *J. Geophys. Res., 96*(C3), 4573-4587, 1991.

Van Aken, H. M., D. Quadfasel, and A. Warpakowski, The arctic front in the Greenland Sea during February 1989: Hydrographic and biological observations, *J. Geophys. Res., 96*(C3), 4739-4750, 1991.

Visbeck, M., J. Fischer, and F. Schott, Preconditioning the Greenland Sea for deep convection: Ice formation and ice drift, *J. Geophys. Res., 100*(C9), 18,489-18,502, 1995.

Visbeck, M., J. Marshall, and H. Jones, Dynamics of isolated convective regions in the ocean, *J. Phys. Oceanogr., 26*, 1721-1734, 1996.

Wackerman, C. C., R. R. Jentz, and R. A. Shuchman, Sea ice type classification of SAR imagery, *IGARSS '88 IEEE Publ. 88CH2497-6*, pp. 425-428, IEEE Press, Piscataway N.J., 1988.

Wadhams, P., J. Comiso, E. Prussen, S. Wells, M. Brandon, E. Aldworth, T. Viehoff, R. Allegrino, and D. Crane, The development of the Odden ice tongue in the Greenland Sea during winter 1993 from remote sensing and field observations, *J. Geophys. Res., 101*(C8), 18,213-18,235, 1996.

K. W. Fischer, C. A. Russel, and R. A. Shuchman, ERIM International Inc., P.O. Box 134008 Ann Arbor, MI 48113-4008.

P. Gloersen, NASA Goddard Space Flight Center, Greenbelt, MD 20771.

J. Johannessen, ESTEC, European Space Agency, 2200 AG, Noordwijk, Netherlands.

O. M. Johannessen, Nansen Environmental and Remote Sensing Center, N-5037 Solheimsviken, Bergen, Norway.

E. G. Josberger, Ice and Climate Project, USGS, University of Puget Sound, Tacoma, WA 98416.

(Received June 28, 1996; revised December 21, 1997; accepted January 23, 1998.)